

Optical and X-ray diffraction characterization of biosynthesis copper oxide nanoparticles using carob leaf extract

Akl M. Awwad*, Qusay Ibrahim

Royal Scientific Society, El Hassan Science City, P.O. Box 1438 Amman 11941 Jordan

*Corresponding author's email: akl.awwad@yahoo.com, phone+962 6 5344701, fax number: +962 6 5344806.

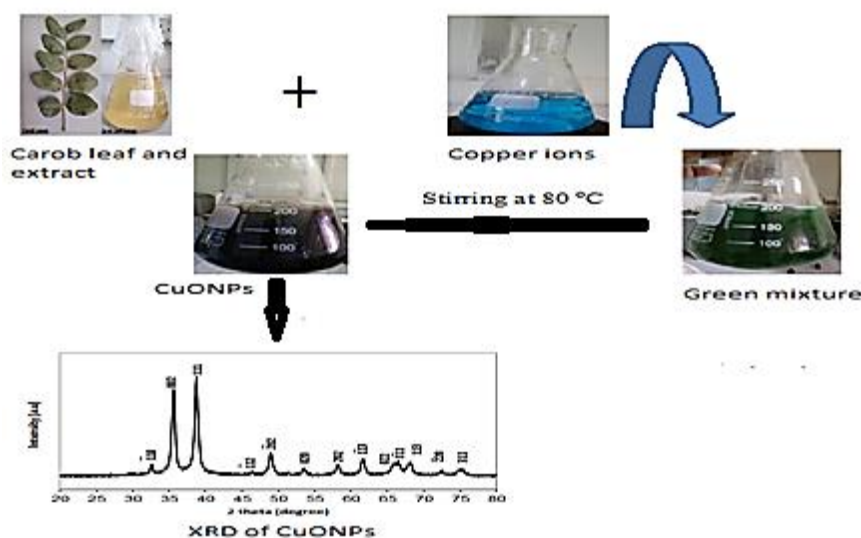
Received 20 November 2014,

Accepted 8 January 2015

Novelty and Highlights:

- 1 – Green synthesis of copper oxide nanoparticles using carob leaf extract.
- 2 – Characterization of copper oxide nanoparticles by UV-vis spectroscopy, SEM, FT-IR, and XRD.
- 3 – The size of copper oxide nanoparticles was in the range 5-20 nm.

Graphical Abstract:



Optical and X-ray diffraction characterization of biosynthesis copper oxide nanoparticles using carob leaf extract

Akl M. Awwad*, Qusay Ibrahim

Royal Scientific Society, El Hassan Science City, P.O. Box 1438 Amman 11941 Jordan,

*Corresponding author's email: akl.awwad@yahoo.com, phone+962 6 5344701, fax number: +962 6 5344806.

Abstract: Copper oxide nanoparticles (CuONPs) have been successfully synthesized from copper acetate monohydrate and carob leaf extract in one pot reaction at 80° C. The biosynthesized copper oxide nanoparticles were characterized by Fourier transform infrared spectroscopy (FT-IR), scanning electron microscopy (SEM), X-ray diffraction (XRD) and UV-vis spectroscopy. The particles are crystalline in nature with average size of 8.0 nm. The morphology of the copper oxide nanoparticles can be controlled by tuning the amount of carob leaf extract and copper ions. This facile and green approach may provide a useful tool to large scale synthesis other nanoparticles that have potential biotechnology.

Keywords: Biosynthesis, copper oxide nanoparticles, carob, Leaf extract, characterization

Introduction

Copper oxide nanoparticles (CuONPs) attracted considerable attention due to their optical, antibacterial, antifungal and conducting properties. Various methods for synthesis of copper oxide (CuONPs) nanoparticles have been achieved via various routes, including sonochemical synthesis [1-3], thermal decomposition method [4], precipitation method [5-7], electrochemical method [8,9], chemical vapor-phase decomposition [10], hydrothermal synthesis [11], reverse micro emulsions [12]. These methods have many disadvantages due to the difficulty of scale up the process of synthesis, separation, purification of the nanoparticles, energy consumption and using hazardous chemicals. Recently, there have been related works employed the potential of green methods to synthesize nanostructures of copper oxide using plant extracts such as *Carcia papaya* leaves extract [13], *Tabernaemontana divaricate* leaf extract [14], tea leaf and coffee powder extracts [15], *Ficus religiosa* leaf extract [16], aqueous extract of *Acalypha indica* [17], *Aloe barbadensis* Miller leaf extract [18], henna leaves [19], *Tabernaemontana divaricate* leaf extract [20], *Centella asiatica* L. leaves extracts [21], flowers of *Cassia alata* [22], and *Terminalia arjuna* leaf extract [23].

The present study was designed with a novel, rapid, cost-effective and environmentally biosynthesis of copper oxide nanoparticles using plant leaf extract of carob as reducing and capping agent. Carob tree grows up to 10 meters in height. The dark green, leathery leaves grow between 10 and 30 cm in length. The alternate, pinnate leaves have 6 to 10 opposite leaflets that are rounded at

the apex. Each leaflet is oval in shape, growing 2 to 8 cm long and 1 to 5 cm broad.

Experimental

Materials Copper acetate monohydrate [Cu (CH₃COO)₂. H₂O] was analytical grade purchased from Merck and used without purification. Distilled and deionized water was used in all experimental work.

Preparation of plant leaf extract Carob leaves were collected from carob trees planted at the campus of Royal Scientific Society, El Hassan Science City, and Amman, Jordan. Leaves were washed several times with distilled water to remove dust particles and then sun dried to remove the residual moisture. Carob leaf extract was prepared by placing 10 g of dried fine cut in 500 ml glass beaker along with 400 ml of sterile distilled water. The mixture was then boiled for 10 minutes until the color of aqueous solution changed from watery to yellow. Then the mixture was cooled to room temperature and filtered with Whatman No. 1 filter paper before centrifuging at 1200 rpm for 2 minutes to remove biomaterials. The extract was stored at room temperature in order to be used for further experiments.

Synthesis of copper oxide nanoparticles (CuONPs) in a typical reaction mixture, 5-10 ml of leaf extract was added drop by drop to 400 ml of 4 mM of aqueous copper acetate monohydrate solution, stirred magnetically at room temperature. As soon as, the leaf extract of carob comes in contact copper ions spontaneous change the blue color of copper ions to green color. Heating and stirred magnetically the obtained green mixture at 80 °C, the green mixture



changed to a reddish brown suspended mixture within one minute, indicating the formation of water soluble monodispersed copper oxide nanoparticles. The concentrations of copper acetate solution and leaf extract were also varied from a 1 to 4 mM and 1% to 10% by volume, respectively.

Characterization techniques scanning electron microscopy (SEM) analysis of synthesized copper oxide nanoparticles was done using a Hitachi S-4500 SEM machine. Powder X-ray diffraction was performed using X-ray diffractometer, Shimadzu, XRD-6000 with $\text{CuK}\alpha$ radiation $\lambda = 1.5405 \text{ \AA}$ over a wide range of Bragg angles ($20^\circ \leq 2\theta \leq 80^\circ$). Fourier transform infrared spectroscopic measurements were done using Shimadzu, IR-Prestige-21 spectrophotometer. UV-vis spectrum of copper oxide nanoparticles was recorded, by taking 0.1 ml of the sample and diluting it with 2 ml deionized water, as a function of time of reaction using a Shimadzu 1601 spectrophotometer in the wavelength region of 300 to 700 nm operated at a resolution of 1 nm.

Results and discussion

XRD pattern revealed the orientation and crystalline nature of copper oxide, Fig. 1. XRD peaks observed at $2\theta = 32.46^\circ, 35.36^\circ, 38.76^\circ, 48.68^\circ, 53.14^\circ, 57.94^\circ, 61.32^\circ, 65.84^\circ, 67.59^\circ, 72.04^\circ,$ and 74.67° corresponding to Bragg's reflection angles 110, -111, 111, -202, 020, 202, -113, 202, -311, 311, and 004, Bragg's reflection based on the crystallinity of copper oxide nanoparticles. All diffraction peaks can be indexed in the CuO monoclinic phase with lattice parameters $a = 0.4685 \text{ \AA}, b = 3.422 \text{ \AA},$ and $c = 5.121 \text{ \AA},$ and $V = 81.14 \text{ \AA}^3,$ which were in good agreement with the standard data from JCPDS 05-0661. No second phase such as copper (I) oxide (Cu_2O) and copper hydroxide, $\text{Cu}(\text{OH})_2$ were found. The mean crystalline sizes of synthesized copper oxide nanoparticles were calculated to be about 8 nm using Debye-Scherrer equation [24]:

$$D = K\lambda / \beta \cos \theta$$

Where D is the crystallite size (nm), K is the shape factor with value from 0.9 to 1, λ is the X-ray wavelength (0.1541 nm), β is the full width at half maximum of the diffraction peak, and θ is the Bragg's angle.

Elemental analysis of the prepared sample of copper oxide nanoparticles (Cu = 78.42% and O = 21.58 %), the weight Cu/O ratio can be calculated to be 3.63, which is very close to the actual ratio of 3.97 for CuO.

The optical characterization of the synthesized copper oxide nanoparticles was recorded on UV-Vis absorption spectrophotometer Fig. 2, in order to determine the band gap energy of copper oxide nanoparticles. The UV-Vis absorption spectroscopy of the sample dissolved in absolute ethanol shows an absorption peak whose center is at about 278 nm. In this study a simple UV-Vis – NIR technique was used to

calculate the band gap energy of synthesized CuONPs and compared with value of bulk CuO.

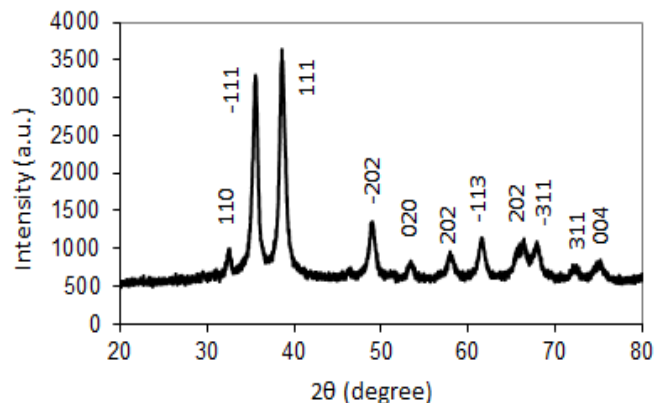


Fig.1. XRD pattern of biosynthesized copper oxide nanoparticles.

The absorption edge energy can be calculated by the following equation [25]:

$$\alpha h\nu = A(h\nu - E_g)^{n/2}$$

where α is the absorption coefficient, h is the Plank's constant, ν is the frequency of the incident photon, E_g is the optical energy direct band gap, A is a constant, and n depends on the nature of transition, equals 1 for direct transition [26]. The band gap estimated by the intercepts of the tangent to the $(\alpha h\nu)^2$ versus photon energy ($h\nu$) as a function of photon energy and extrapolating the linear portion of the curve to the photon energy axis. From the plot, Fig. 3, the direct energy band gap was estimated to be 3.2 eV.

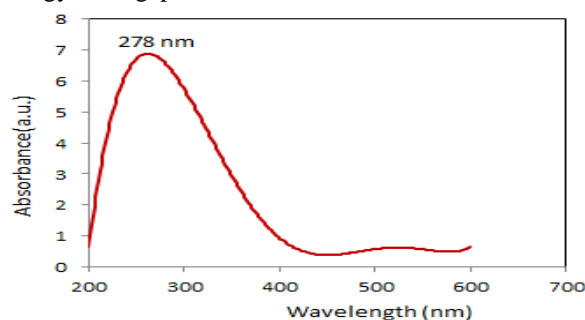


Fig.2. UV-vis absorption spectra of synthesized copper oxide nanoparticles using carob leaf extract.

FT-IR analysis is used to identify and get approximate ideas of the possible biomolecules that are responsible for reducing copper ions and stabilizing the synthesized CuONPs with the carob leaf extract. The spectrum obtained for carob leaf extract showed bands at 3406, 2920, 2850, 1725, 1612, 1539, 1446, 1377, 1199, 1022, 740, and 555 cm^{-1} , Fig.4. A strong peak at 3406 cm^{-1} can be attributed hydrogen bonded O-H groups of alcohols and phenols and also to the presence of amines N-H of amide in carob leaf extract. This peak shifted to higher field at 3414 cm^{-1} in the carob-CuONPs. The bands at 2920 cm^{-1} and 2850 cm^{-1} are assigned to $-\text{CH}_2$ and C-H

stretching mode in alkanes. The shoulder peak at 1725 cm^{-1} in carob leaf extract could be attributed to C=C stretching vibrations about C=O amide conjugated C=O of the proteins that are responsible for reducing and capping CuONPs. The peaks at 1612 , 1539 , and 1446 cm^{-1} represent the carbonyl stretching of -C=O , aromatic stretching of -C-N and -O-C-O .

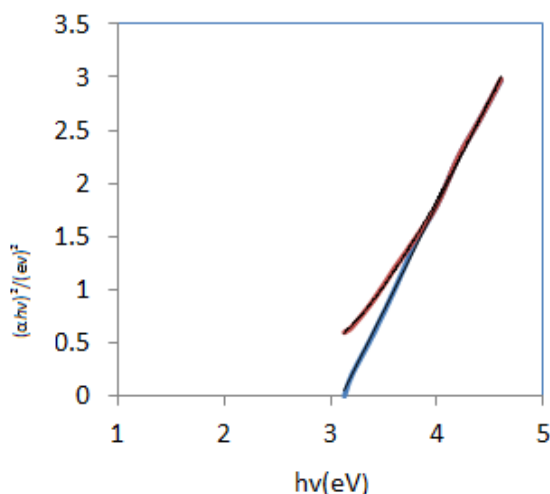


Fig. 3. $(Ahv)^2$ - $h\nu$ curve of the copper oxide nanoparticles.

The bands at 740 cm^{-1} and 555 cm^{-1} indicated the presence of R-CH group and C-H bending. The shifting in the stretching observed in carob-CuONPs (Fig. 5) at 3406 , 1612 , 1446 , and 1377 cm^{-1} indicated that the functional groups including phenol, aromatic amine and carbonyl groups from carob mediated the reduction and capping of carob-CuONPs.

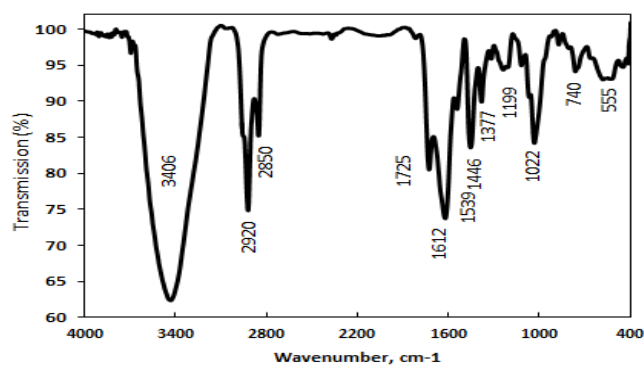


Fig.4. FT-IR spectra of carob leaf extract.

The existence bands at 598 , 497 , and 428 cm^{-1} are recognized to Cu-O vibrations and confirming the formation of CuONPs. Overall the results of microscopy and spectroscopy suggest that proteins in carob leaf extract can act as reducing and capping agent and thus protect the nanoparticles from agglomeration in the aqueous medium. Comparison between spectra of carob leaf extract sample and carob-CuONPs

sample reveal changes in the positions as well as on the magnitude of the biosorption bands.

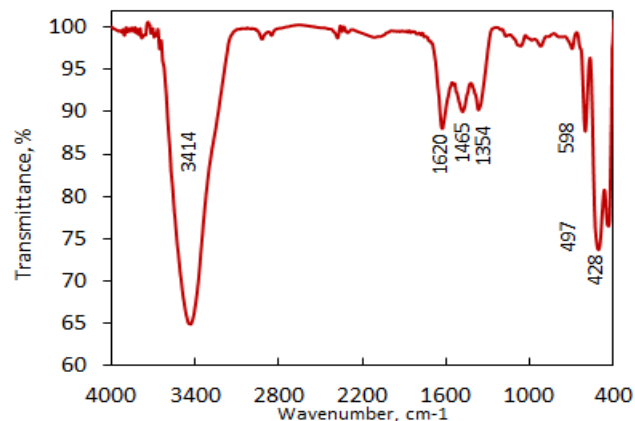


Fig.5. FT-IR spectra of the biosynthesized copper oxide nanoparticles using carob leaf extract.

The SEM image of copper oxide nanoparticles was spherical in shape with evenly distributed throughout the colloidal solution, Fig. 6. The SEM observation showed the presence of agglomerated nanospheres with an average diameter of $5\text{--}20\text{ nm}$. This slight deviation of the particle size estimation compared to that calculated from XRD analysis can be attributed to the deviation of the spherical shape of the particles that is required for the Debye-Scherrer formula and the detection limit of the XRD diffractometer.

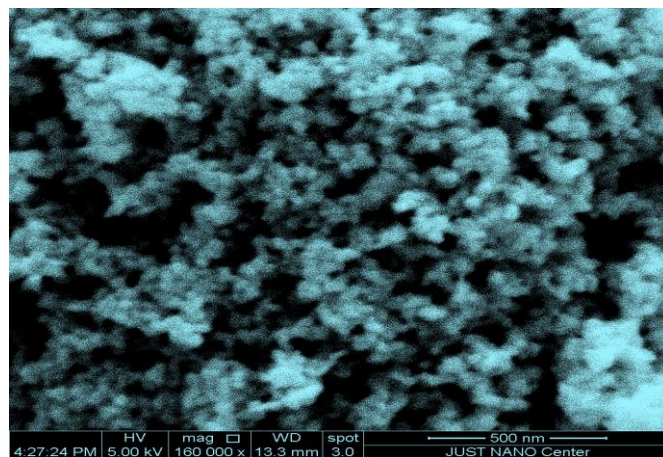


Fig.6. SEM image of biosynthesized CuONPs using carob leaf extract.

Conclusions

A new and green method has been developed for synthesis copper oxide nanoparticles CuONPs in one pot reaction process at 80°C . Our synthesis approach employed an environmental friendly biomaterial, carob leaf extract, as an alternative to organic solvents and

surfactants. Carob leaf extract acts as reducing, capping and stabilizing agent, which prevents the agglomeration of copper oxide nanoparticles formed during synthesis. XRD and SEM data showed that the size and shape of nanoparticles could be controlled by the amount of carob leaf extract and the concentration of Cu(II) ions. Spherical and polydispersed CuONPs of particle sizes ranging from 5 to 20 nm with an average size of 8 nm are obtained. The method of the present study offers several important advantageous features. First, the synthesis route is economical and environmentally friendly; because it involves inexpensive and non-toxic materials. Second, large scale synthesis

Acknowledgements

Authors are grateful to Royal Scientific Society, El Hassan Science City for providing all facilities to carry out this research work.

Notes and references

1. N. Wongpisutpaisan, P. Charoonsuk, N. Vittayakorn, W. Pecharapa. *Energy Procedia* 2011, **29**, 404.
2. V. Safarifard, A. Morsali. *Ultrasonics Sonochemistry* 2012, **19**, 823.
3. A. Shui, W. Zhu, L. Xu, D. Qin, Y. Wang, *Ceramics International* 2013, **39**, 8715.
4. E. Darezereshki, F. Bakhtiari. *J. Min. Metall. Sect. B-Metall.* 2011, **47**, 73.
5. K. Phiwdang, S. Suphankij, W. Mekprasart, W. Pecharapa, *Energy Procedia* 2013, **34**, 740.
6. A. Rahnam, M. Gharagozlou. *Optical and Quantum Electronics* 2012, **44**, 313.
7. M. Sahooli, S. Sabbaghi, R. Saboori. *Mater. Lett.* 2012, **81**, 169.
8. P. Pandey, S. Merwyn, G.S. Agarwal, B.K. Tripathi, S.C. Pant. *J. Nanopart. Res.* 2012, **14**, 709.
9. S. Jadhav, S. Gaikwad, M. Nimse, A. Rajbhoj. *Journal of Cluster Science* 2011, **22**, 121.
10. A.G. Nasibulin, L.I. Shurygina, E.I. Kauppinen. *Colloid Journal* 2005, **67**, 1.
11. M. Outokesh, M. Hosseinpour, S.J. Ahmadi, T. Mousavand, S. Sadjadi, W. Soltanian. *Ind. Eng. Chem. Res.* 2011, **50**, 3540.
12. A. Kumar, A. Saxena, A. De, R. Shankar, S. Mozumdar, *RSC Adv.* 2013, **3**, 5015.
13. R. Sankar, P. Manikandan, V. Malarvizhi, T. Fathima, K. S. Shivashangari, V. Ravikumar. *Spectrochim. Acta A* 2014, **121**, 746.
14. R. sivaraj, P.K.S.M. Ramasn, P. Rajiv, H.A. Salam, R. Venckatesh, *Spectrochim. Acta A* 2014, **133**, 178.
15. P. Sutradhar, M. Saha, D. Maiti, *J. Nanostruct. Chem.* 2014, **4**, 86.
16. R. Sankar, R. Maheswari, S. Karthik, K.S. Shivashangari, V. Ravikumar, *Mater. Sci. Eng. C* 2014, **44**, 234.
17. R. sivaraj, P.K.S.M. Ramasn, P. Rajiv, S. Narendhram, R. Venckatesh, *Spectrochim. Acta A* 2014, **129**, 255.
18. S. Gunalan, R. Sivaraj, R. Venckatesg, *Spectrochim. Acta A* 2012, **97**, 1140.
19. K. Cheirmadurai, S. Biswas, R. Murali, P. Thanikaivelan, *RSC Adv.* 2014, **4**, 19507.
20. R. Sivaraj, P.K.Rahman, P. Rajiv, H.A. Salam, R. Venckatesh, *Spectrochim. Acta A* 2014, **133**, 178.
21. H.S. Devi, T.D. Singh, *Advance in Electronic and Electric Engineering* 2014, **4**, 83.
22. Jayzlakshmi, A. Yogamoorthi. *Inter. J. Nanomater. Biostruct.* 2014, **4**, 66.
23. S. Yallappa, J. Manjanna, M.A. Sindhe, N.D. Satyanarayan, S.N. Pramod, K. Nagaraja. *Spectrochim. Acta A* 2013, **110**, 108.
24. H.P. Klug, L.E. Alexander, *X-ray diffraction procedures*, Wiley, New York, 1959.
25. M. Umadevi, A.J. Christy, *Spectrochim. Acta A* 2013, **109**, 133.
26. M. Kaur, K.P. Muthe, S.K. Despande, S. Choudhury, J.B. Singh, N. Verma. *J. Cryst. Growth* 2006, **289**, 670.